ISSN 1674-1056
http://cpb.iphy.ac.cn
http://iopscience.iop.org/cpb
中国物理 B
Chinese Physics
中国物理 Chinese Physics B

First polar direct-drive exploding-pusher target experiments on the ShenGuang laser facility

Bo Yu(余波), Jiamin Yang(杨家敏), Tianxuan Huang(黄天晅), Peng Wang(王鹏), Wanli Shang(尚万里), Xiumei Qiao(乔秀梅), Xuewei Deng(邓学伟), Zhanwen Zhang(张占文), Zifeng Song(宋仔峰), Qi Tang(唐琦), Xiaoshi Peng(彭晓世), Jiabin Chen(陈家斌), Yulong Li(理玉龙), Wei Jiang(蒋炜), Yudong Pu(蒲昱东), Ji Yan(晏骥), Zhongjing Chen(陈忠靖), Yunsong Dong(董云松), Wudi Zheng(郑无敌), Feng Wang(王峰), Shaoen Jiang(江少恩), Yongkun Ding(丁永坤), Jian Zheng(郑坚)
Citation: Chin. Phys. B . 2019, 28(9): 095203 . **doi:** 10.1088/1674-1056/28/095203
Journal homepage: http://cpb.iphy.ac.cn; http://iopscience.iop.org/cpb

What follows is a list of articles you may be interested in

Influence analysis of symmetry on capsule in six-cylinder-port hohlraum

You Zou(邹游), Wudi Zheng(郑无敌), Xin Li(李欣)
Chin. Phys. B . 2019, 28(3): 035203 . **doi:** 10.1088/1674-1056/28/3/035203

Coupling between velocity and interface perturbations in cylindrical Rayleigh-Taylor instability

Hong-Yu Guo(郭宏宇), Li-Feng Wang(王立锋), Wen-Hua Ye(叶文华), Jun-Feng Wu(吴俊峰), Wei-Yan Zhang(张维岩)
Chin. Phys. B . 2018, 27(5): 055205 . **doi:** 10.1088/1674-1056/27/5/055205

Rayleigh-Taylor instability at spherical interfaces of incompressible fluids

Hong-Yu Guo(郭宏宇), Li-Feng Wang(王立锋), Wen-Hua Ye(叶文华), Jun-Feng Wu(吴俊峰), Ying-Jun Li(李英骏), Wei-Yan Zhang(张维岩)
Chin. Phys. B . 2018, 27(2): 025206 . **doi:** 10.1088/1674-1056/27/2/025206

A new ignition hohlraum design for indirect-drive inertial confinement fusion

Xin Li(李欣), Chang-Shu Wu(吴畅书), Zhen-Sheng Dai(戴振生), Wu-Di Zheng(郑无敌), Jian-Fa Gu(谷建法), Pei-Jun Gu(古培俊), Shi-Yang Zou(邹士阳), Jie Liu(刘杰), Shao-Ping Zhu(朱少平)
Chin. Phys. B . 2016, 25(8): 085202 . **doi:** 10.1088/1674-1056/25/8/085202

Effect of inner-surface roughness of conical target on laser absorption and fast electron generation

Wang Huan, Cao Li-Hua, Zhao Zong-Qing, Yu Ming-Yang, Gu Yu-Qiu, He Xian-Tu
Chin. Phys. B . 2014, 23(5): 055202 . **doi:** 10.1088/1674-1056/23/5/055202

First polar direct-drive exploding-pusher target experiments on the ShenGuang laser facility*

Bo Yu(余波)[1,2,†], Jiamin Yang(杨家敏)[1], Tianxuan Huang(黄天暄)[1], Peng Wang(王鹏)[1], Wanli Shang(尚万里)[1], Xiumei Qiao(乔秀梅)[3], Xuewei Deng(邓学伟)[1], Zhanwen Zhang(张占文)[1], Zifeng Song(宋仔峰)[1], Qi Tang(唐琦)[1], Xiaoshi Peng(彭晓世)[1], Jiabin Chen(陈家斌)[1], Yulong Li(理玉龙)[1], Wei Jiang(蒋炜)[1], Yudong Pu(蒲昱东)[1], Ji Yan(晏骥)[1], Zhongjing Chen(陈忠靖)[1], Yunsong Dong(董云松)[1], Wudi Zheng(郑无敌)[3], Feng Wang(王峰)[1], Shaoen Jiang(江少恩)[1], Yongkun Ding(丁永坤)[2,3], and Jian Zheng(郑坚)[2,4]

[1] *Laser Fusion Research Center, China Academy of Engineering Physics, Mianyang* 621900, *China*
[2] *Department of Modern Physics, University of Science and Technology of China, Hefei* 230026, *China*
[3] *Institute of Applied Physics and Computational Mathematics, Beijing* 100088, *China*
[4] *IFSA Collaborative Innovation Center, Shanghai Jiao Tong University, Shanghai* 200240, *China*

(Received 7 May 2019; revised manuscript received 21 July 2019; published online 30 August 2019)

Low density and low convergence implosion occurs in the exploding-pusher target experiment, and generates neutrons isotropically to develop a high yield platform. In order to validate the performance of ShenGuang (SG) laser facility and test nuclear diagnostics, all 48-beam lasers with an on-target energy of 48 kJ were firstly used to drive room-temperature, DT gas-filled glass targets. The optimization has been carried out and optimal drive uniformity was obtained by the combination of beam repointing and target. The final irradiation uniformity of less than 5% on polar direct-drive capsules of 540 μm in diameter was achieved, and the highest thermonuclear yield of the polar direct-drive DT fuel implosion at the SG was 1.04×10^{13}. The experiment results show neutron yields severely depend on the irradiation uniformity and laser timing, and decrease with the increase of the diameter and fuel pressure of the target. The thin CH ablator does not impact the implosion performance, but the laser drive uniformity is important. The simulated results validate that the $\cos\gamma$ distribution laser design is reasonable and can achieve a symmetric pressure distribution. Further optimization will focus on measuring the symmetry of the hot spot by self-emission imaging, increasing the diameter, and decreasing the fuel pressure.

Keywords: polar direct-drive, exploding-pusher target, neutron yield, irradiation uniformity

PACS: 52.57.–z, 52.57.Fg, 29.25.Dz, 02.60.Pn **DOI:** 10.1088/1674-1056/ab37f4

1. Introduction

The direct-drive exploding pusher target experiments[1–3] were designed to develop a high neutron yield platform before the cryogenic system is operational. The exploding pusher implosions are directly heated by laser, drive a strong shock wave into the fuel, and produce fusion reactions. Strong-shock implosions[4] have been demonstrated to be insensitive to the drive-asymmetry and have one dimension feature. Such excellent platform has the advantages of monoenergetic neutron or proton, and is usually used to develop the nuclear diagnostic system and to study the nuclear and plasma processes. When D^3He gas is imploded,[5,6] the implosion works as monoenergetic proton backlighting[7,8] to study the high-energy-density phenomena in both basic science and inertial confinement fusion, such as self-generated fields,[9] Rayleigh–Taylor instability growth,[10] etc.

High convergence, direct drive implosions require spherically uniform irradiation to reduce the hydrodynamic instabilities.[11] The overall nonuniformity should be less than 1% root-mean-square, depending on the number of beams and the beam placement. The sufficient, symmetrical beam distribution, like in the Omega Laser Facility,[12] is suitable for the direct drive implosions. In order to perform the direct drive experiment on the indirect drive laser facility, the polar direct-drive[13] (PDD) has been proposed. PDD repoints some of the beams toward the polar or equator of the target to achieve the most-uniform irradiation. The repointed beams are more obliquely incident on the target, and have lower laser absorption and less laser–target coupling efficiency, thereby the higher laser energy is required and the more complexity pulse shapes are employed to satisfy the drive uniformity. Nevertheless, the energy coupling efficiency to the fuel of the PDD approach is higher than that of the indirect drive. The PDD proof-of-principle experiments[14] were demonstrated on OMEGA using the 40-beam subset without the equatorial beams.

The direct drive exploding pusher implosions are proposed to produce high neutron yields from the beginning of laser fusion.[11] The long wavelength laser was used in the early exploding-pusher experiments, but the low laser absorption[15] and high fuel preheat precluded high compression. The exploding pusher implosions at Nova[16] and

*Project supported by the National Natural Science Foundation of China (Grant No. 11605178) and the Science Challenging Project, China (Grant Nos. JCKY2016212A505 and TZ2016001).
†Corresponding author. E-mail: yubobnu@163.com
© 2019 Chinese Physical Society and IOP Publishing Ltd

Omega[1] were developed to high neutron yield sources for neutron diagnostic development. The neutron yield up to 1.4×10^{14} makes Omega have the chance to study the anomalous degradation in yield with ^{3}He addition,[17] calibrate the differential cross section for the elastic n–^{2}H and n–^{3}H scatterings,[18] test the effect of pre-mix Ar and Xe,[19] and measure the stopping of energetic D^{3}He protons in warm dense plasma.[20] The National Ignition Facility[21] (NIF) PDD experiments began with exploding-pusher capsules to generate a large amount of neutrons and protons for diagnostic calibration purpose. It was also used to develop the nuclear science platform[22,23] to probe the ion kinetic effects,[24,25] infer mixed mass,[26,27] and study the nuclear reaction relevant to stellar nucleosynthesis[28] and big-bang nucleosynthesis.[2]

This article introduces our first PDD, DT fuel implosion experiments on the ShenGuang (SG) laser facility.[29] The experiments imploded some room-temperature gas-filled glass capsules with 1 ns square pulse. The experimental neutron yields exceeded 10^{13}, and severely depended on the irradiation uniformity, laser timing, diameter and fuel pressure of the target. We start with the introduction of the SG laser facility, beam repointing strategy, and experiment details. Then the first implosion experiment results of nuclear diagnostic are described. Finally, the discussions and conclusions are made.

2. Initial experiments design

The PDD experiments were carried on the SG laser facility.[29] SG is designed with 48 laser beams which are distributed over four cones per hemisphere, at polar angles $\theta = 28.5^\circ$, 35°, 49.5°, and 55° referred to the target chamber axis, as shown in Fig. 1. The numbers of beams uniformly distributed in each cone are 4, 4, 8, 8, respectively, on each side. The adjacent cones of 28.5° and 35° are tilted by 45°, the adjacent cones of 49.5° and 55° are tilted by 22.5°, and the cones between two hemispheres are tilted by 22.5°.

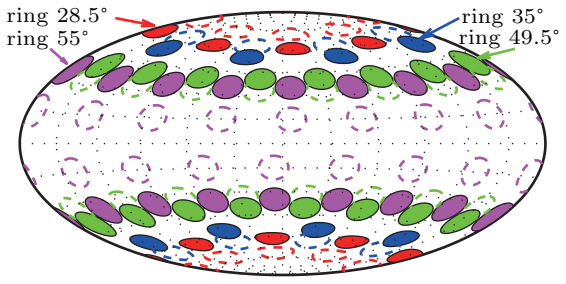


Fig. 1. The SG beam configuration. All beams are arranged in four rings per hemisphere ($\theta = 28.5^\circ$, 35°, 49.5°, 55°). Solid circle: original place; dashed circle: repointed place.

The SG facility is designed for indirect-drive inertial confinement fusion research and can deliver more than 100 kJ of ultraviolet light ($\lambda = 351$ nm, 3ω of Nd laser) within 3 ns pulse duration. When the laser is used for direct-drive implosion, the beam centerlines should be realigned and the beam power should be adjusted to improve the implosion uniformity to acceptable levels. The optimized repointing is to move the inner cones to polar and the outer cones to equator, which increases the drive energy on the capsule's polar and equator, as shown in Fig. 2.

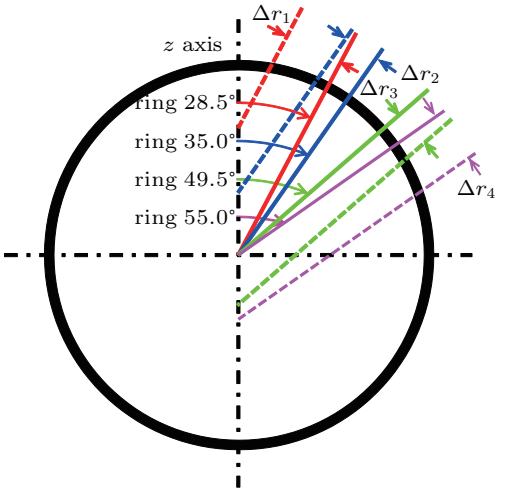


Fig. 2. The laser beam repointing strategy. Laser beams are moved to polar or equator to increase the drive energy on the capsule's polar or equator. $\Delta r_1, \Delta r_2, \Delta r_3, \Delta r_4$ are the repointing distances reference to the axes of lasers. Solid lines: original beams; dashed lines: repointed beams.

The continuous phase plate (CPP) smoothing technique[30] has been used in the SG facility, and it is expected to produce a uniform circular intensity profile with the diameter 500 μm at the laser entrance holes. Thereby the laser beams have ellipse cross sections with different minor axes in different cones. The incidence angle is larger, the minor axis of the laser spot is shorter, and the cross section is more oblate.

The laser intensity profile $I(x,y)$ can be described by super-Gaussian[31]

$$I(x,y) = I_0\,\mathrm{e}^{-(\sqrt{x^2+(y/\cos\theta)^2}/\delta)^n},$$

where n is the order, approximately 5 on the SG facility, and δ is the 1/e radius of the laser spot, $\delta = 211$ μm for the radius 250 μm of the laser spot. The PDD experiments were driven with approximately 1 kJ/1 ns/beam, the laser intensity of each beam was 0.9–1.4×10^{15} W/cm^2. The incidence angle is larger, the size of the laser spot is smaller, and the laser intensity is higher, as shown in Fig. 3.

When the ratio of laser-spot size to target diameter is reduced to below 0.8, the neutron yields rapidly decrease despite increasing absorbed energy.[32] Thus the initial implosion experiments were performed on glass-shell capsules with diameters $\sim$ 540 μm and glass wall thickness $\sim$ 2.6 μm. The capsules were overcoated with parylene (μm-thickness) and filled with $\sim$ 40 atm of equal-molar DT gas at room temperature, as shown in Fig. 4(a). The driving laser was square pulses with 1 ns duration and 120 ps rise time (10%–90%), as shown in Fig. 4(b).

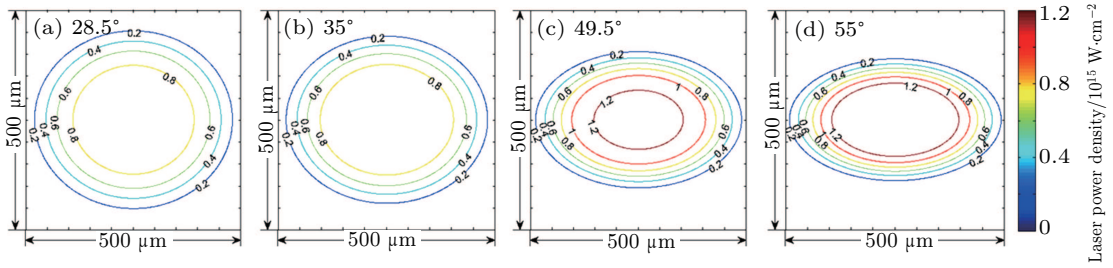


Fig. 3. The laser intensity distribution of each cone, related to the angle of laser incident. The highest intensity of each beam is 0.9–1.4 × 10^{15} W/cm^2.

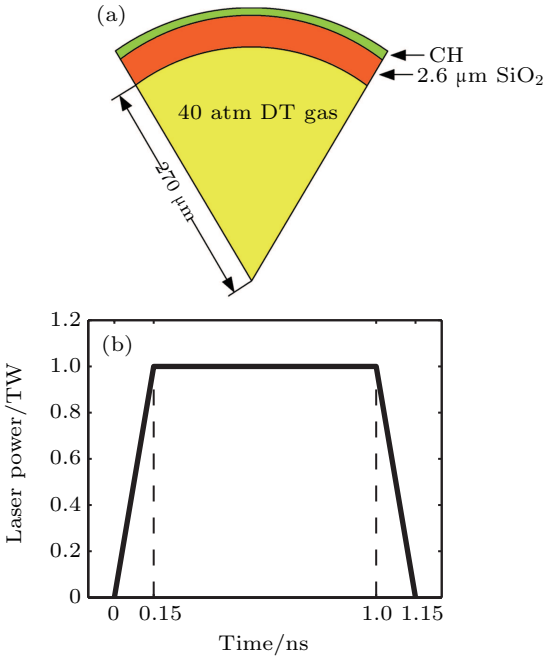


Fig. 4. (a) The target for PDD exploding-pusher experiments and (b) pulse shape.

To minimize the irradiation nonuniformity and optimize the repointing distances, 3D view factor method,[33] an analytical geometry method, was used to rapidly evaluate the root-mean-square deviation of the laser intensity over the target. It assumes that energy deposition is related to the angle of normal (γ) on the target surface to compensate reduced absorption at the polar or equator, where laser beam trajectories are seriously diverted when a plasma corona develops. The principle of the maximum utilization of laser energy and the minimum cross of laser beam were also employed, the centers of laser beams were limited in the corresponding hemisphere where lasers irradiated on.

As the first PDD experiments on the SG facility, the laser beams were repointed, the laser power and pulse shape were not adjusted. Two different distribution assumptions of the energy deposition were employed. Firstly, the energy deposition is given by a $\cos^2\gamma$ distribution,[34] the repointing distance from the center of the capsule is $-51/-29/47/116$ μm for Φ540 μm capsule, and the irradiation nonuniformity on the target is 4.30%, as shown in Fig. 5(a). Secondly, the energy deposition is supposed to have a $\cos\gamma$ distribution, the repointing distance is $-51/-36/35/99$ μm for Φ540 μm capsule, and the irradiation nonuniformity on the target is 3.49%, as shown in Fig. 5(b). The experimental parameters wre optimized according to the target diameter by 3D view factor code.

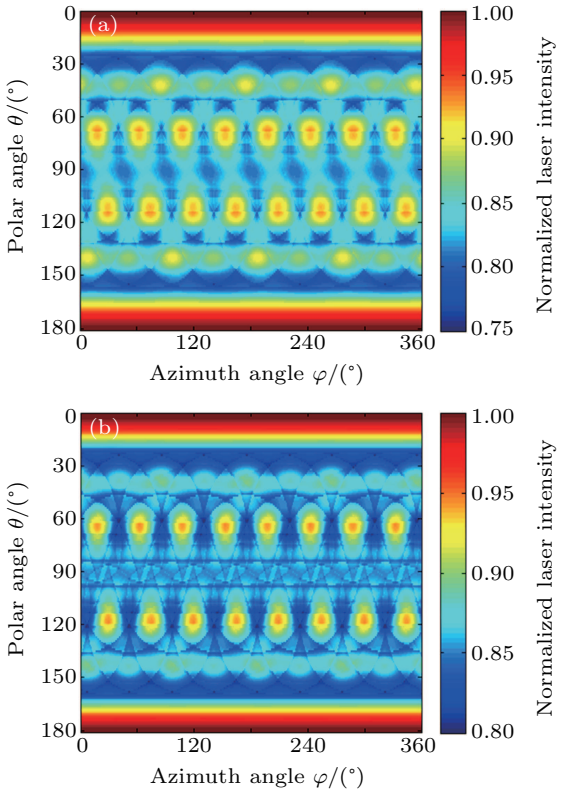


Fig. 5. The irradiation uniformity on Φ540 μm capsule with (a) $\cos^2\gamma$ or (b) $\cos\gamma$ distribution of the energy deposition. The laser intensity is normalized.

Three nuclear diagnostics were used to measure the neutron yield, ion temperature, and neutron bang time in our first PDD experiments. Optical and x-ray diagnostic systems were not used because of the pollution of tritium. The copper activation system,[35] which was calibrated at an accelerator, was used to absolutely measure the primary neutron yield. The Φ7 cm × 1 cm copper sample was located at 82 cm from the target chamber center (TCC). The ion temperature was measured by a neutron time-of-flight (nTOF) detector.[36] The nTOF detector, composed of a plastic scintillator and fast photomultiplier tubes, was placed at 10–13 m from TCC. The neutron fu-

sion reaction rate diagnostic system[37] based on the fast plastic scintillator and optical streak camera measured the neutron bang time and fusion reaction rate history. The 2 mm-thin fast plastic scintillator (EJ232) was placed at a 3 cm distance from TCC and acted as a neutron-to-light converter. The time response of the detector is less than 30 ps.

3. Experiment results

CH ablator targets of different thicknesses, including 0 μm, 1 μm, 1.8 μm, were imploded in the experiments and the majority of shots were implemented with $\cos^2\gamma$ distribution design. After the major work of nuclear physics application was finished under the stable neutron yield, the last shot (20151227103) was tried to improve the neutron yield and experimented with $\cos\gamma$ distribution design. Figure 6 shows the neutron yield accurately measured by the copper activation system.[35] The highest neutron yield was 1.04×10^{13}, imploded with $\cos\gamma$ distribution of the energy deposition in the last shot.

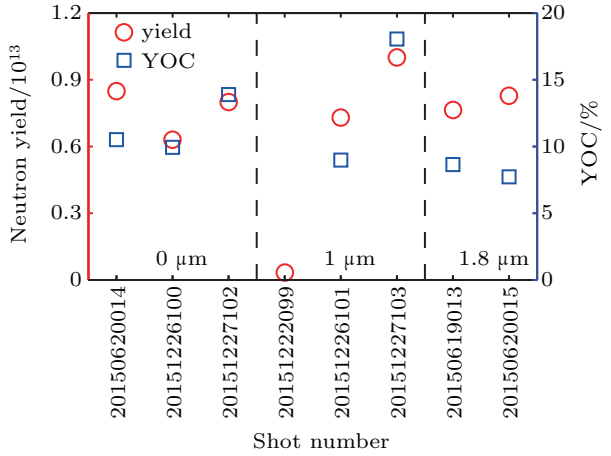


Fig. 6. The neutron yield measured by copper activation system. YOC is between 5% and 20%. Shot 20151227103 was imploded with $\cos\gamma$ distribution, other shots were imploded with $\cos^2\gamma$ distribution.

The neutron yield was very small in the shot 20151222099 (3.4×10^{11}), far below from the simulated yield. After carefully checking the characters of the facility, the laser timing was found to be the key problem. Figure 7 shows the statistic results of laser timing based on the temporal waveform recorded with the oscillographs. The statistic results reveal the considerable fluctuation of the laser timing. The maximum error of laser timing was larger than 200 ps and not acceptable for the exploding-pusher experiment. In order to renew the timing of each beam, a fast photomultiplier tube was placed at TCC to measure the arriving time of each beam. The statistic fluctuation of the improved timing was smaller than 20 ps.

The ratio of the neutron yield to the 1D prediction yield over clean (YOC) was 5%–20%. The clean yields were simulated by hydrodynamics code Muli1D[38] with a flux limiter of 0.03 and local heat transport model. The last four shots were firstly simulated because of the only obtained results of neutron bang time shown in Fig. 8, and the laser absorption efficiency was adjusted to make the simulated neutron bang time accord with the measured neutron bang time. The simulated results of the last four shots show that the average absorption efficiency is 20%. Then, other shots were simulated with the same laser absorption efficiency.

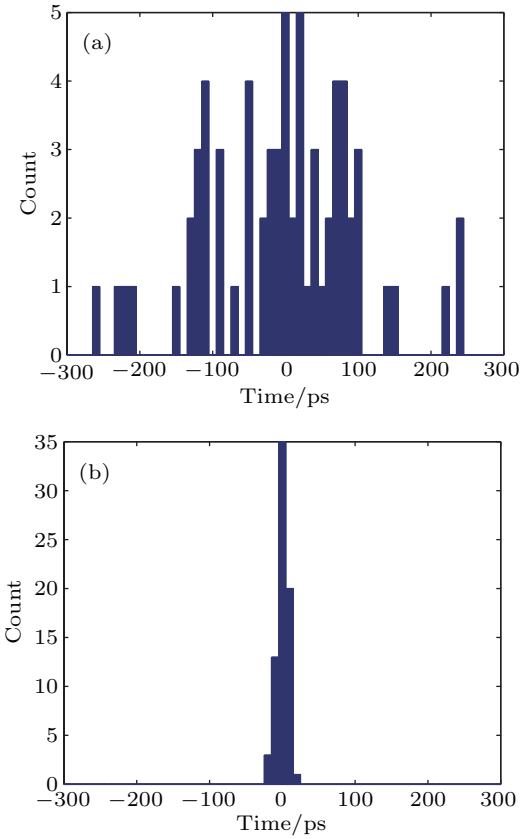


Fig. 7. The statistic results of two shots: (a) before and (b) after the laser timing was regulated. The maximum error was larger than 200 ps before the laser timing was modulated.

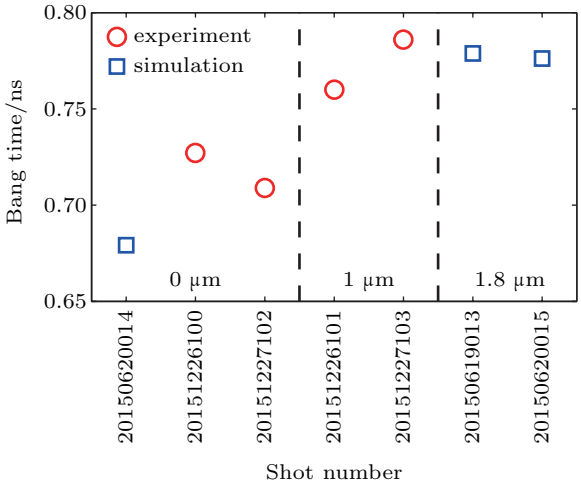


Fig. 8. Neutron bang time measured by neutron fusion reaction rate diagnostic system. Only the last four shots were available and presented.

The neutron bang time was measured by the neutron fusion reaction rate diagnostic system.[37] The available results were only obtained at the last four shots. After neutron signal extraction and time-based correction, information of the neutron bang time is encoded in the leading edge of the pulse, as shown in Fig. 8. The experimental results of neutron bang time are 0.7–0.8 ns and burn width are 120–160 ps.

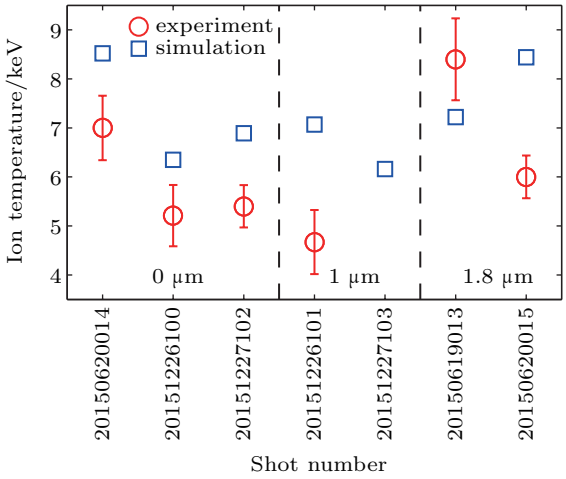


Fig. 9. Ion temperature measured by nTOF detector. Shot 20151227103 is missed because of the malfunction of the nTOF detector.

The ion temperature was deduced from the nTOF spectrum.[36] The measured results of ion temperature except the last shot are shown in Fig. 9. The ion temperatures range from 4 keV to 9 keV. The fluctuation is remarkably larger than that of neutron yields. The discrepancy of ion temperature between predicted and observed is also noticeable, and the experimental results are smaller than the simulated results, probably caused by the bad symmetry at the $\cos^2\gamma$ distribution assumption. Of course, the ion kinetic effects may also become remarkably in our experiments. The hydrodynamics processes with consideration of ion and electron nonlocal heat transport[39,40] are expected for the more detailed simulations.

4. Discussion

The neutron yields of the exploding pusher target were stable between 6×10^{12} and 1×10^{13}, though the thickness of the CH ablator was slightly changed. Because the density of glass was higher than the CH density, the implosion performance of Φ540 μm target was dominated by the thickness of glass, not evidently impacted by the thin CH ablator, even if the thickness was 1.8 μm. The experiments validated that the PDD exploding-pusher target experiment is a robust high neutron yield platform, capable of producing yields up to 10^{13} DT neutron for laser energy 48 kJ.

The highest neutron yield was observed at the second repointing assumption. This assumption moves more laser energy to polar to increase the irradiation. Without other changes of experimental condition, the experimentally increased neutron yield in the second assumption revealed the improved implosion symmetry. In order to simulate the improvement of symmetry, the hydrodynamics code Multi2D[41] was used. Multi2D includes Lagrangian hydrodynamics, diffusive heat transport, and laser deposition. Laser deposition is modeled with 3D ray tracing algorithm including refraction and absorption by classical inverse bremsstrahlung, but not crossed-beam energy transport. Figures 10(a) and 10(b) show the 2D hydrodynamics simulated results of CH of 1 μm. The pressure distribution of the hot spot is obviously improved for the second assumption, indicated that the laser drive is significantly stronger on the equator than on the polar at the first repointing assumption. The simulated results will be directly confirmed by measuring self-emission images with time-resolved x-ray imaging[42] in the later experiment.

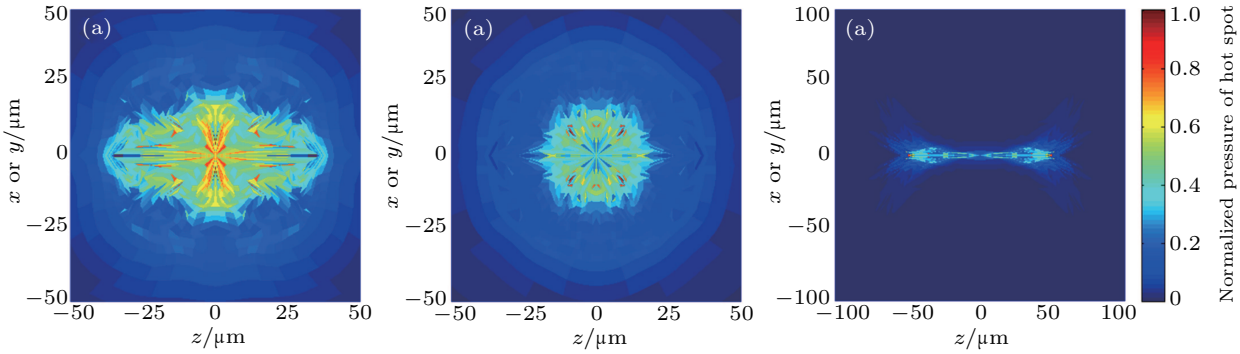


Fig. 10. Pressure distribution of hot spot: (a) $\cos^2\gamma$ (shot 20151226101), (b) $\cos\gamma$ (shot 20151227103), and (c) laser mistiming in the shot 20151222099.

The neutron yield of the shot 20151222099 was very small, the laser timing was found to be the key reason. The timing fluctuation can be also considered as the bad symmetry. For the direct drive, the considerably fluctuation of the laser timing makes the time discrepancy of the strong shock produced at the glass shell, then the shock cannot arrive at the center of the target at the same time, and the gas fuel cannot be compressed and heated enough when the shock rebounds back through the fuel. The diverge shock wave produces little of fusion reaction. Figure 10(c) shows the semi-quantitative sim-

ulated result of laser mistiming. The laser mistiming of each ring was 40/30/60/−60 ps, which is the statistic from the laser waveforms. The pressure distribution of the hot spot is more oblate than that in Fig. 10(a), the reason is that the laser of the equator arrived ahead on the target.

The laser drive uniformity is also important for the direct drive exploding pusher implosion, it can be indirectly validated from Fig. 11(a). The neutron yields decreased evidently when the diameter of the target became bigger at the first repointing assumption. In general, the diameter is smaller, the overlap of the laser beams is more sufficient, the irradiation uniformity is better, and the neutron yield is higher.

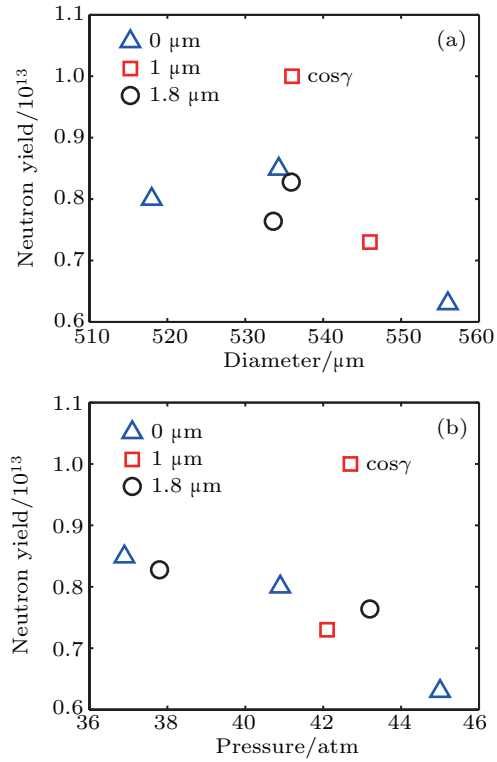


Fig. 11. Measured neutron yield as a function of (a) the diameter and (b) the gas pressure of the target. One shot was imploded with $\cos\gamma$ assumption, the other shots were imploded with $\cos^2\gamma$ assumption.

The neutron yield is also related with the fuel pressure, as shown in Fig. 11(b). The neutron yield is seen to descend over the fuel pressure, consistent with the experiment results at Omega.[2] The fuel of low pressure can be compressed easily, and the yields are decided by the fuel areal densities.

The neutron yields of exploding pusher target experiments were lower than the desired yields. The neutron yield of 10^{13} is not enough high for the nuclear physics application, such as neutron imaging system, the signal noise ratio is only 7 dB for glass capillaries with 200-μm-diameter, located at 13 m away. A minimum of 10^{14} neutrons are required, the signal noise ratio will be improved to 20 dB. The target parameters are firstly optimized, and the optimizations have been focused on the diameter and fill pressure. According to the experiment results, 1 ns square laser pulse with energy 48 kJ, laser absorption efficiency of 20%, flux limiter of 0.03, and local heat transport were used in the Multi1D[38] simulation. Limited by the mature technology of glass shell production, three diameters with fixed shell thickness and different fill pressures were simulated. The simulated results are shown in Fig. 12. The optimal target is Φ720 μm with 5–10 atm gas and the neutron yield is three times higher than that of the current target. The potential risk of Φ720 μm target is that the ratio of laser-spot size to target diameter is below 0.7, the irradiation uniformity becomes worse and the neutron yield may decrease.

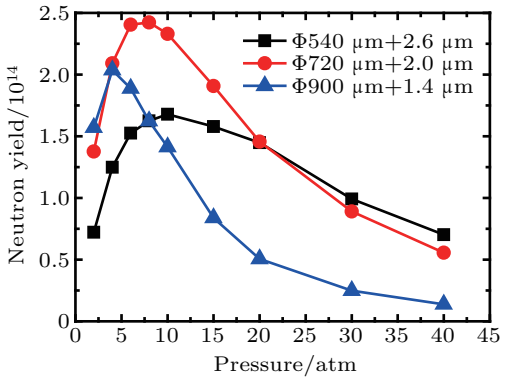


Fig. 12. Neutron yield from Multi1D simulation with three diameters and different fill pressures of glass target.

The simulated results generally reproduce the experiment trends shown in Fig. 11. The neutron yields climb with the increase of diameter for 40 atm fuel pressure, and drop with the decrease of fuel pressure for Φ540 μm target.

5. Conclusion

The SG laser facility is initially designed for the indirect-drive implosion experiments with 48 laser beams. The laser beams need be repointed to improve drive uniformity when PDD implosion experiments are carried out. By using a set of optimized repointing parameters to increase the drive on the capsule's polar and equator, the final irradiation nonuniformity was less than 5% on PDD capsules of 540 μm in diameter.

In the first PDD experiments, the thin-glass shell targets were used. The operation capability of the SG facility was tested and demonstrated. When the capsules were $\sim$ 540 μm in diameter with $\sim$ 2.6 μm-thick glass shell, filled with $\sim$ 40 atm DT gas at room temperature, the experimental neutron yield up to 10^{13} and ion temperature up to 9 keV have been observed. Up to now, it is the highest neutron yield in China ICF experiments.

Nuclear diagnostics, including the copper activation system, nTOF detector, and neutron fusion reaction rate diagnostic system have demonstrated high performance in excess of their specifications in the PDD experiments. With the implementation of these nuclear diagnostics, the dependence of the

neutron yields on irradiation uniformity, laser timing, diameter and fuel pressure of target were investigated in our experiments. The results show that the larger diameter and lower fuel pressure of the target are in favor of increasing neutron yields.

Higher yield requirement of minimum of 10^{14} urges to further optimize the target parameters, including the diameter and fill pressure. Another direction under investigation is to optimize repointing by including the effects of mispointing, power imbalance, and study the effects of beam smoothing and pulse shaping.

Acknowledgment

The authors would like to thank the staffs of the target fabrication and the SG laser facility for their cooperation.

References

[1] Soures J M, McCrory R L, Verdon C P, *et al.* 1996 *Phys. Plasmas* **3** 2108
[2] Johnson M G, Zylstra A B, Bacher A, *et al.* 2017 *Phys. Plasmas* **24** 041407
[3] Ellison C L, Whitley H D, Brown C R D, *et al.* 2018 *Phys. Plasmas* **25** 072710
[4] Rygg J R, Frenje J A, Li C K, *et al.* 2008 *Phys. Plasmas* **15** 034505
[5] Miles A R, Chung H K, Heeter R, *et al.* 2012 *Phys. Plasmas* **19** 072702
[6] Rosenberg M J, Zylstr A B, Séguin F H, *et al.* 2016 *High Energy Dens. Phys.* **18** 38
[7] Manuel M J E, Zylstra A B, Rinderknecht H G, *et al.* 2012 *Rev. Sci. Instrum.* **83** 063506
[8] Rygg J R, Zylstra A B, Séguin F H, *et al.* 2015 *Rev. Sci. Instrum.* **86** 116104
[9] Li C K, Seguin F H, Frenje J A, *et al.* 2010 *Science* **327** 1231
[10] Manuel M J E, Li C K, Séguin F H, *et al.* 2012 *Phys. Rev. Lett.* **108** 255006
[11] Craxton R S, Anderson K S, Boehly T R, *et al.* 2015 *Phys. Plasmas* **22** 110501
[12] Boehly T R, Brown D L, Craxton R S, *et al.* 1997 *Opt. Commun.* **133** 495
[13] Skupsky S, Marozas J A, Craxton R S, *et al.* 2004 *Phys. Plasmas* **11** 2763
[14] Craxton R S, Marshall F J, M J Bonino, *et al.* 2005 2005 *Phys. Plasmas* **12** 056304
[15] Garban-Labaune C, Fabre E, Max C E, *et al.* 1982 *Phys. Rev. Lett.* **48** 1018
[16] Campbell E M, Ploeger W M, Lee P H, *et al.* 1980 *Appl. Phys. Lett.* **36** 965
[17] Herrmann H W, Langenbrunner J R, Mack J M, *et al.* 2009 *Phys. Plasmas* **16** 056312
[18] Frenje J A, Li C K, Séguin F H, *et al.* 2011 *Phys. Rev. Lett.* **107** 122502
[19] Dodd E S, Benage J F, Kyrala G A, *et al.* 2012 *Phys. Plasmas* **19** 042703
[20] Zylstra A B, Frenje J A, Grabowski P E, *et al.* 2015 *Phys. Rev. Lett.* **114** 215002
[21] Haynam C A, Wegner P J, Auerbach J M, *et al.* 2007 *Appl. Opt.* **46** 3276
[22] Rinderknecht H G, Sio H, Li C K, *et al.* 2014 *Phys. Plasmas* **21** 056311
[23] Rosenberg M J, Rinderknecht H G, Hoffman N M, *et al.* 2014 *Phys. Rev. Lett.* **112** 185001
[24] Rosenberg M J, Zylstra A B, Séguin F H, *et al.* 2014 *Phys. Plasmas* **21** 122712
[25] Rinderknecht H G, Amendt P A, Rosenberg M J, *et al.* 2017 *Nucl. Fusion* **57** 066014
[26] Rinderknecht H G, Rosenberg M J, Zylstra A B, *et al.* 2015 *Phys. Plasmas* **22** 082709
[27] Larroche O, Rinderknecht H G and Rosenberg M J 2018 *Phys. Rev. E* **98** 031201
[28] Casey D T, Sayre D B, Brune C R, *et al.* 2017 *Nat. Phys.* **13** 1227
[29] Zheng W G, Wei X F, Zhu Q H, *et al.* 2017 *Matter Radiat. At. Extremes* **2** 243
[30] Yang C L, Zhang R Z, Xu Q, *et al.* 2008 *Appl. Opt.* **47** 1465
[31] Weilacher F, Radha P B, Collins T J, *et al.* 2015 *Phys. Plasmas* **22** 032701
[32] Froula D H, Igumenshchev I V, Michel D T, *et al.* 2012 *Phys. Rev. Lett.* **108** 125003
[33] Basko M 1996 *Phys. Plasmas* **3** 4148
[34] Ramis R, Temporal M, Canaud B, *et al.* 2014 *Phys. Plasmas* **21** 082710
[35] Song Z F, Tang Q, Chen J B, *et al.* 2015 *High Power Laser Part. Beams* **27** 112005 (in Chinese)
[36] Chen J B, Zheng Z J, Peng H S, *et al.* 2001 *Rev. Sci. Instrum.* **72** 3534
[37] Wang F, Peng X S, Kang D G, *et al.* 2013 *Chin. Phys. B* **22** 115204
[38] Ramis R, Schmalz J and Meyer-ter-Vehn J 1988 *Comput. Phys. Commun.* **49** 475
[39] Schurtz G P, Nicolai P D and Busquet M 2000 *Phys. Plasmas* **7** 4238
[40] Zhao B, Hu G Y, Zheng J, *et al.* 2018 *High Energy Dens. Phys.* **28** 1
[41] Ramis R, Meyer-ter-Vehn J and Ramireza J 2009 *Comput. Phys. Commun.* **180** 977
[42] Cao Z R, Miao W Y, Dong J J, *et al.* 2012 *Acta Phys. Sin.* **61** 075213 (in Chinese)